Exploring the niche concept in a simple metaorganism

Peter Deines[1]*, Katrin Hammerschmidt[2] and Thomas CG Bosch[1]

[1]Zoological Institute, Christian-Albrechts-University Kiel, 24118 Kiel, Germany
[2]Institute of General Microbiology, Christian-Albrechts-University Kiel, 24118 Kiel, Germany

*Correspondence:
Peter Deines
pdeines@zoologie.uni-kiel.de

Abstract
Organisms and their resident microbial communities - the microbiome - form a complex and mostly stable ecosystem. It is known that the composition of the microbiome and bacterial species abundances can have a major impact on host health and *Darwinian fitness*, but the processes that lead to these microbial patterns have not yet been identified. We here apply the niche concept and trait-based approaches as a first step in understanding the patterns underlying microbial community assembly and structure in the simple metaorganism *Hydra*. We find that the carrying capacities in single associations do not reflect microbiota densities as part of the community, indicating a discrepancy between the fundamental and realized niche. Whereas in most cases, the realized niche is smaller than the fundamental one, as predicted by theory, the opposite is observed for *Hydra*'s two main bacterial colonizers. Both, *Curvibacter* sp. and *Duganella* sp. benefit from association with the other members of the microbiome and reach higher fractions as compared to when they are the only colonizer. This cannot be linked to any particular trait that is relevant for interacting with the host or by the utilization of specific nutrients but is most likely determined by metabolic interactions between the individual microbiome members.

Keywords
fundamental niche, realized niche, microbiome, species abundance, microbial traits, *Hydra*

Running title
Microbial traits, niches, and the metaorganism

Number of words: 5263
Number of figures: 6

Introduction

Microbiomes contribute to ecosystems as key engines that power system-level processes (Falkowski et al., 2008). This also applies to host ecosystems, where they are critical in maintaining host health, survival, and function (Kau et al., 2011; McFall-Ngai et al., 2013). Despite their importance, the mechanisms governing microbiome assembly and composition are largely unknown. This is different for macroscopic communities, thanks to the application of niche (Holt, 2009; Leibold, 1995; Whittaker et al., 1973) and trait-based theories, which might also provide a useful framework for studying the ecology and evolution of microbiomes in metaorganisms (Kopac and Klassen, 2016).

The niche concept is one of the core concepts in ecology and has been rediscovered by modern ecology for explaining biodiversity and species coexistence patterns (Pocheville, 2015). The niche-based theory states that an ecological community is made up of a limited number of niches, each occupied by a single species. Hutchinson (Hutchinson, 1957) defined the *fundamental niche* as the needs of a species for it to maintain a positive population growth rate, disregarding biotic interactions (Hutchinson, 1957; Pearman et al., 2008). The fundamental niche therefore represents an idealized situation exclusive of interspecific interactions. The effect of biological interactions is taken into account in the definition of the *realized niche* (Hutchinson, 1957). This is the portion of the fundamental niche in which a species has a positive population growth rate, despite the constraining effects of biological interactions, such as inter-specific competition (Hutchinson, 1957; Pearman et al., 2008).

In the last two decades, the shift from taxonomy to function by using trait-based approaches has provided a detailed understanding of biodiversity-ecosystem functioning (Louca et al., 2018). Recently, this framework is also being used by microbial ecologists to study microbial biogeography (Green et al., 2008), or to unravel microbial biodiversity-ecosystem functioning relationships (Krause et al., 2014). Further, this approach allows studying microbiomes in the light of coexisting traits/ functions rather than of coexisting microbes (Martiny et al., 2015). A recent study successfully used this approach and analyzed trait-based patterns to understand the mechanisms of community assembly and succession of the infant gut microbiome (Guittar et al., 2019). Microbial traits cover a range of phenotypic characteristics, for example organic phosphate utilization, bacteriophage host range, cellulose degradation, biofilm formation, nitrogen fixation, methanogenesis, and salinity preference (Martiny et al., 2015). Potential microbial traits can be measured directly by laboratory assays (as in this study) or can be indirectly inferred based on genomic information.

The aim of this study is to apply the niche concept and trait-based theory to the metaorganism *Hydra vulgaris* (strain AEP) to gain insight into the mechanisms underlying the microbial community composition. We thus specifically extend the niche-assembly perspective, classically used for assessing species assembly and coexistence in abiotic environments, to a host-associated microbiome, thus a biotic environment.

The freshwater polyp *Hydra* and its microbiome have become a valuable model system for metaorganism research as it provides a bridge between the simplicity of synthetic communities and the complex mouse model (Deines and Bosch, 2016). The ectoderm is covered by a multi-layered glycocalyx, which is the habitat for a highly stable, low complexity, species specific microbiome (Bosch, 2013; Deines et al., 2017; Franzenburg et al., 2013), with a carrying capacity of

$1.7*10^5$ CFUs per *Hydra* (Deines et al., 2020). The six most abundant bacterial colonizers of *Hydra vulgaris* (strain AEP) make up between 84 - 90% of *Hydra*'s microbiome (Franzenburg et al., 2013; Murillo-Rincón et al., 2017). These species, *Curvibacter* sp. (65 - 76%), *Duganella* sp. (11 - 16%), *Undibacterium* sp. (1 - 2%), *Acidovorax* sp. (0.4 - 0.7%), *Pseudomonas* sp. (0.4%), and *Pelomonas* sp. (0.2 - 0.9%), were isolated and purified by Fraune et al. (2015). The single-species isolates can be cultured and manipulated *in vitro* (Bosch, 2013; Fraune et al., 2015; Wein et al., 2018), allowing the measurement of phenotypic microbial traits and fitness. Fitness, as defined by niche theory, is the positive population growth of the focal species, which in our study is that of the six available microbiome members. Measurements of the performance of the bacterial populations when grown singly, i.e. in the absence of the other microbial competitors *in vitro* and *in vivo* (on germ-free *Hydra* polyps), specify the fundamental niche. For each species, we compare the fundamental niche to the realized niche, which we calculated based on published data on the microbiome composition of wild-type and conventionalized polyps (germ-free polyps incubated with tissue homogenates of wild-type animals) (Franzenburg et al., 2013; Murillo-Rincón et al., 2017). We also measure phenotypic traits that might be connected to the success of the various microbial species in occupying the fundamental niche; these are essentially traits that might play a role in successfully populating their environment, the host, such as biofilm formation, surface hydrophobicity (bacterial cells are more likely to attach to surfaces with the same hydrophobicity), and nutrient utilization patterns. Here we focused on carbon sources as the microbiome inhabits the outer mucus-like layer of *Hydra*'s glycocalyx (Fraune et al., 2015), which is carbohydrate-rich (Ouwerkerk et al., 2013; Schröder and Bosch, 2016). As the realized niche is determined by biological interactions of one species with its associate microbial community, we focus on traits that are important when competing with other species, such as growth rate, niche overlap, and niche breadth. Ultimately, we take the traits and the ecological niches as determinants of species interactions, which may infer the assembly and structure of the host-associated microbiome.

Materials and Methods

Animals used, culture conditions, and generation of germ-free animals

Hydra vulgaris (strain AEP) was used in the experiments and cultured according to standard procedures at 18°C in standardized *Hydra* culture medium (Lenhoff and Brown, 1970). Animals were fed three times a week with 1st instar larvae of *Artemia salina*. Germ-free polyps were obtained as previously described (Franzenburg et al., 2013; Murillo-Rincón et al., 2017). After two weeks of treatment, polyps were transferred into antibiotic-free sterile *Hydra* culture medium for recovery (four days). Sterility was confirmed by established methods (Franzenburg et al., 2013). During antibiotic treatment and re-colonization experiments, polyps were not fed.

Bacterial species and media

The bacterial species used in this study are *Curvibacter* sp. AEP1.3, *Duganella* sp. C1.2, *Undibacterium* sp. C1.1, *Acidovorax* sp. AEP1.4, *Pelomonas* sp. AEP2.2, and *Pseudomonas* sp. C2.2 (all Gammaproteobacteria), all of which were isolated from the *Hydra vulgaris* (strain AEP) microbiome (Fraune et al., 2015). These bacteria were cultured from existing isolate stocks in R2A medium at 18°C, shaken at 250 r.p.m for 72 h before use in the different experiments.

Fundamental and realized niche

Germ-free polyps (n=18) were inoculated with single bacterial species using $5x10^3$ cells in 1.5 ml Eppendorf tubes containing 1 ml of sterile *Hydra* culture medium (each n=3). After 24 h of incubation, all polyps were washed with, and transferred to sterile *Hydra* culture medium, incubated at 18°C. After three days of incubation individual polyps were homogenized in an Eppendorf tube using a sterile pestle, after which serial dilutions of the homogenate were plated on R2A agar plates to determine colony-forming units (CFUs) per polyp (Deines et al., 2020). The dilution with counts in the countable range was selected for each bacterial species, counting a minimum of 50 CFUs per plate.

The carrying capacities of mono-associations provide information of the occupied niche space on the host in the absence of other microbial species that are part of the microbiome, and thus specifies the fundamental niche for each (as calculated from the proportion of each species from the sum of all).

As microbial community composition and relative microbial abundances of wild-type and conventionalized polyps have been reported to be remarkably stable over time (Bosch, 2013; Franzenburg et al., 2013; Fraune et al., 2015; Murillo-Rincón et al., 2017), we here base the estimates of the realized niche on the underlying original data from previous studies (Franzenburg et al., 2013; Murillo-Rincón et al., 2017). For OTU (operational taxonomic unit) estimations of *Hydra*'s microbiome, both studies used amplicon sequencing of the variable regions 1 and 2 (V1V2) of the bacterial 16S rRNA genes (V1V2-one step approach). The sequences were grouped into OTUs at a $\geq$ 97% sequence identity threshold. For the relative abundance estimates, all samples were normalized to the lowest number of reads in each respective dataset. Note that it has been shown for *Hydra*'s microbiome that relative abundance estimations based on 16S rRNA amplicon sequencing do not significantly differ compared to relative abundance estimations based on metagenomic shotgun sequencing (Rausch et al., 2019).

Carrying capacities of the members when part of the full community could not be assessed via plating of the community as was done for the mono-associations as not all bacterial species can be differentiated based on colony morphology, which is

why we based calculations of the realized niche on data that was previously published (Franzenburg et al., 2013; Fraune et al., 2015; Murillo-Rincón et al., 2017). Other studies demonstrate that germ-free polyps, which were inoculated with the natural community of species (conventionalized animals), harbor an equally dense microbiome (CFUs per polyp; Deines et al., 2020) that is remarkably similar in its composition (Murillo-Rincón et al., 2017) as compared to wild-type polyps. This indicates that the generation and re-exposure of germ-free animals does not lead to an overall change in carrying capacity or community composition.

Cell surface hydrophobicity (CSH)

The BATH assay was performed as described previously (Borecká-Melkusová and Bujdáková, 2008; Rosenberg, 1984). It uses a biphasic separation method to measure cell surface hydrophobicity. In short, for each species tested, exponential growth phase cultures of the six species were adjusted to an optical density at 600nm (OD_{600}) of 0.1 in R2A medium ($OD_{initial}$). 4 ml of this bacterial suspension was placed into a glass tube, overlaid with 1 ml of n-hexodecane (Sigma Aldrich), and vortexed for 3 min. The phases were then allowed to separate for 15 min, after which the ODs of the aqueous (lower) phase containing hydrophilic cells was measured at OD_{600} ($OD_{residual}$). The hydrophobic cells are found in the n-hexodecane overlay (upper phase). OD values were compared to the bacterial suspension before mixing with n-hexodecane. The relative hydrophobicity (RH) was calculated as follows: RH = $((OD_{initial} - OD_{residual})/OD_{initial})$ x 100%. The experiment was performed in triplicate with independent bacterial overnight cultures.

Biofilm quantification by use of crystal violet (CV)

Biofilm formation was assayed and quantified as previously described (Ren et al., 2015). Briefly, exponential growth phase cultures of the six species were adjusted to an OD_{600} = 0.1 in R2A medium. Biofilm formation was assayed in a 96 well plate using four replicates for each treatment inoculated from the same bacterial overnight culture. For single isolates an inoculation volume of 180 µl was used. After 48 h of incubation at 18°C with shaking (200 r.p.m) biofilm formation was quantified by a modified crystal violet (CV) assay (Peeters et al., 2008).

Characterizing nutrient (carbon) utilization

To characterize the nutrient profiles, specifically the carbon metabolism profile, for each species of *Hydra*'s microbiota, we used BIOLOG GN2 plates. BIOLOG GN2 plates are 96-well microwell plates containing 95 different carbon sources plus a carbon-absent water control well. Species were grown from isolate stocks in R2A medium (18°C, shaken at 250 r.p.m.), centrifuged at 3000 r.c.f. for 5 min, re-suspended in S medium and adjusted to an OD_{600} of 0.1. Each well of the BIOLOG plate was inoculated with 150 µl of bacterial suspension and incubated for three days at 18°C in a humid chamber. Growth on each of the 95 nutrients was determined as OD_{600} of each well using a TECAN plate reader. For each plate, the OD of the water control was subtracted from the reading of all other wells prior to analysis, and differenced OD values below 0.005 were considered as no growth (Vaz Jauri et al., 2013). Nutrient use was evaluated on three replicate plates inoculated from independent bacterial overnight cultures. Nutrient niche overlap (NO) was calculated using the formula: NO = (number of nutrients used by both A and B)/((number of nutrients used by A + number of nutrients used by B)/ 2) (Vaz Jauri et al., 2013). A value of 1 indicates the use of the same nutrients (100% overlap) and 0 indicates no

228 nutrient overlap among the 95 substrates tested. We also calculated the relative use of
229 the eleven functional groups (carbohydrates, carboxylic acids, amino acids, polymers,
230 aromatic chemicals, amines, amides, phosphorylated chemicals, esters, alcohols and
231 bromide chemicals) according to Daou et al. (2017). In brief, the relative use of C
232 substrates was calculated as absorption values in each well divided by the total
233 absorption in the plate.
234
235 **Measurement of bacterial growth rates *in vitro***
236 Cultures of the all six species were produced in R2A microcosms (grown for 72 h at
237 18°C, at 250 r.p.m). Aliquots of each culture were first washed in S medium and then
238 re-suspended in fresh R2A medium to an optical density of 0.025 at 600 nm (OD_{600}).
239 Growth kinetics of all species were determined in 96-well microtiter plates. A 100 µl
240 aliquot of each re-suspension was pipetted into 100 µl of fresh R2A medium. The
241 microtiter plate was then placed in a microplate reader (TECAN Spark 10M, Tecan
242 Group Ltd., Switzerland), and the OD_{600} of each well was measured at 30 min
243 intervals for 96 cycles (with 10 sec shaking at 150 r.p.m. prior to each read). The
244 growth of each species was determined in five well locations on an individual 96-well
245 plate, which was replicated six times with independent bacterial overnight cultures.
246 The maximum growth rate (μ_{max}) was calculated from the maximum slope of the
247 absorbance over time.
248
249 **Statistical analysis**
250 Analysis of variance (ANOVA) and subsequent post hoc Tukey-Kramer tests were
251 used to test for differences in the carrying capacity of the six *Hydra* colonizers. To
252 meet the requirements for the model, the variable was Box-Cox transformed. A
253 Welch ANOVA (and subsequent Wilcoxon post hoc tests) was used to test for
254 differences in the fraction of the different species in the community, differences in
255 biofilm formation capacity, and *in vitro* growth rates between the species.
256 Analysis of variance (ANOVA) and subsequent post hoc Tukey-Kramer tests were
257 used to test for differences in the cell surface hydrophobicity of the six *Hydra*
258 colonizers.
259 Sample size was chosen to maximise statistical power and ensure sufficient
260 replication. Assumptions of the tests, that is, normality and equal distribution of
261 variances, were visually evaluated (see Quinn and Keough, 2003, for rationale). Non-
262 significant interactions were removed from the models. Effects were considered
263 significant at the level of $P < 0.05$. All statistical analyses were performed with JMP
264 9. Graphs were produced with GraphPad Prism 5.0, and RStudio (RStudio Team,
265 2015).
266

Results

Fundamental and realized niche occupation of the different bacterial species

In mono-colonizations, the six bacterial species differ significantly in their carrying capacity on *Hydra* (Figure 1A; ANOVA: $F_{5,12}$=12.696, P=0.0002). The most extreme cases are *Acidovorax* sp. that reaches the highest numbers with $2.6*10^5$ CFUs/polyp, and *Duganella* sp. the lowest with $1.7*10^4$ CFUs/polyp. Mono-colonization of *Acidovorax* sp. thus exceeds the carrying capacity of the wild-type microbiome of $1.7*10^5$ CFUs per *Hydra* (Deines et al., 2020). Based on the carrying capacity of the single species in mono-colonisations, we estimated the fundamental niche of each of the six species. The realized niche of the six bacterial species is calculated based on previously published data on the composition of the extremely stable microbial community. The species differed in their relative abundance as part of the microbial community (Figure 1B; Welch ANOVA: $F_{5,14}$=86.722, P<0.0001). The most dominant species is *Curvibacter* sp. representing 65% of the microbial community, followed by *Duganella* sp. that reaches about 16%. All other four species reach only comparatively low fractions (around 1%), with *Acidovorax* sp. being the lowest. When comparing the fundamental to the realized niche (Figure 2), we find that the realized niche of *Curvibacter* sp. and *Duganella* sp. is larger than their fundamental niche. This is in contrast to all other species, where as expected by theory, competition with other microbes leads to a smaller realized than the fundamental niche.

Bacterial traits

Associated with occupation of the fundamental niche

The BATH assay was conducted with six species of the *Hydra* microbiome to measure cell surface hydrophobicity (CSH). The CSH of the bacterial species vary, with values ranging from 0% to 42% and significantly differing between species (ANOVA: $F_{5,12}$=26.869; P<0.0001). *Curvibacter* sp. and *Pelomonas* sp. were the only two species that did not show any affinity to the hexadecone; thus their cell population can be considered homogeneous consisting of only hydrophilic cells, which significantly differs from the others, except for *Pseudomonas* sp. (Figure 3A). *Pseudomonas* sp. and *Undibacterium* sp. show a mixed cell population, where 10 to 20% of the cells are hydrophobic. The species with the highest percentage of hydrophobic cells are *Acidovorax* sp. and *Duganella* sp., between 30 and 35%.

The species differed in their biofilm formation (Welch ANOVA: $F_{5,18}$=350.723, P<0.0001). All species formed biofilms (Figure 3B), with *Pelomonas* sp. producing the largest biomass amount, which significantly differed from all other species. The biofilm amount of *Acidovorax* sp. was also significantly different from all other species but only roughly a third of the mass that *Pelomonas* sp. produced. All other species did not differ and are comparatively weak biofilm producers.

Nutrient utilization, i.e. carbon substrate usage, of all species was determined using a BIOLOG assay. The 94 carbon substrates are organized into eleven functional groups (Figure 4). Results showed that all six species actively oxidize carbon compounds such as carbohydrates (30-50% relative use), carboxylic acids (15-35% relative use) and amino acids (15-35% relative use) (Figure 4; Figure 5A). Carbohydrates are being used to an equal extent between all species, except for *Undibacterium* sp., which uses the highest amount of around 50% (relative use). Turanose is the compound most highly utilised, followed by a-D-lactose, L-rhamnose, and D-cellobiose. The use of carboxylic acids increases in the species, which are characterized by low frequencies in the *Hydra* microbiome, with the exception of

Duganella sp. (with a relative use of 25-30%). Here D-galactonic acid lactone is the substrate with the highest usage, followed by different forms of hydroxyl butyric acids. Amino acids are most excessively used by *Acidovorax* sp., *Curvibacter* sp. and *Pseudomonas* sp., whereas the other species use amino acids to a lesser extent. Polymers are being used very differently between the species with *Pseudomonas* sp. showing the highest and *Undibacterium* sp. the lowest values. Amines are being used more frequent by the dominant species in the microbiome and are utilized to a lesser extent by the low abundant species.

Associated with occupation of the realized niche

When comparing the *in vitro* growth rates we find species perform differently (Figure 3C; Welch ANOVA: $F_{5,174}$=223.856, P<0.0001). The fastest species, *Undibacterium* sp., grows twice as fast as compared to the slowest one, *Pelomonas* sp..

The overlap in carbon substrate usage between all six microbiome members is displayed as a Venn diagram (Figure 5B). There are only two substrates, which are not utilized by any species, whereas 20 substrates are used by all species. There are only two species that can metabolize substrates that none of the other species is using. While *Pseudomonas* sp. uses two substrates: i-erythritol and lactulose, *Curvibacter* sp. is able to utilise eight substrates: D-arabitol, D-mannose, D-trehalose, mono-methyl succinate, formic acid, glucuronamide, L-pyroglutamic acid, and D-serine. The number of substrates shared exclusively between two species only is between one and two.

Niche overlap (NO) among all pairwise species combinations ranged from 60 to 80% (Figure 5C). *Curvibacter* sp. shares the highest overlap (80%) with *Pseudomonas* sp. and *Duganella* sp.. For the other species the overlap ranges between 60 and 70%. *Duganella* sp. displays the highest overlap with *Pseudomonas* sp. and *Undibacterium* sp. around 80%, whereas the overlap between *Pelomonas* sp. and *Acidovorax* sp. reaches almost 70%. *Undibacterium* sp. exhibits an overlap of 60 to 70% with *Acidovorax* sp., *Pseudomonas* sp. and *Pelomonas* sp.. *Acidovorax* sp. a 80% overlap with *Pseudomonas* sp. and 70% overlap with *Pelomonas* sp.. *Pseudomonas* sp. and *Pelomonas* sp. show a 75% overlap of the nutrients used. Mean niche overlap was determined as the mean of all pairwise niche overlap values for each species. Comparing the number of nutrients being used by the individual species we find that *Curvibacter* sp. and *Pseudomonas* sp. are able to use 70% of the provided substrates. *Duganella* sp. uses 57%, *Acidovorax* sp. 54% and *Pelomonas* sp. 51%. The lowest substrate utilization was measured for *Undibacterium* sp. with 41% of the available substrates.

Discussion

Microbial communities residing in abiotic environments typically comprise numerous interacting species. Such communities have been studied with traditional approaches, for example the niche-assembly concept, which is an extension of the classical niche theory (Hutchinson, 1957). The niche-assembly perspective proposes that any ecosystem is made up of a limited number of niches, each occupied by a single species (Wennekes et al., 2012). Thus, the partitioning of these niches leads to the stable coexistence of competing species within an ecosystem. To assess the rules of assembly and coexistence of microbiota in host-associated microbiomes, we here apply the niche-assembly perspective to a metaorganism, and thus specifically extend the concept to biotic environments.

We find that the fundamental niche (here defined by the absence of interspecific microbial interactions) differs considerably from the realized niche of *Hydra*'s associated microbes (Figure 2). This reflects the difference in performance between the species when they individually occupy *Hydra* (mono-association) as to when they occur as part of their microbial community on the host. As predicted by niche theory, we find for the majority of the species that the realized niche is smaller than the fundamental one, most likely caused by interspecific microbial competition, as has also been observed in other systems, e.g. *Vibrios* in their marine environment (Materna et al., 2012). In our study, the best colonizer in the mono-colonizations, *Acidovorax* sp. (as also observed by Fraune et al. (2015)), is the least abundant species as part of the microbial community. While we cannot provide details on the nature of the interspecific competition within the whole community as observed here, a recent study investigated the interaction between the two main *Hydra* colonizers, *Curvibacter* sp. and *Duganella* sp., in more detail (Deines et al., 2020). While *Duganella* sp. likely benefitted from products excreted by *Curvibacter* sp., it was able to outcompete *Curvibacter* sp. in the tested *in vitro* environments (but not on the host). Most importantly, this effect was independent of initial frequency but depended on direct contact, which might be due to competition for the same resources or due to *Duganella* sp. actively harming *Curvibacter* sp., e.g. through contact-depending killing (see Granato et al., 2019 for an overview on potential mechanisms). In the host context, a stable co-occurrence might be achieved through spatial segregation of microbial colonizers or through active manipulation by *Hydra*, for example through the secretion of antimicrobial peptides and neuropeptides (Franzenburg et al., 2013; Augustin et al., 2017). Nevertheless, when part of the whole microbial community, both main colonizers in the community, *Curvibacter* sp. and *Duganella* sp., occupy a much bigger realized niche than fundamental niche. This finding is very interesting and indicates that the two species benefit from interactions when part of the whole microbiome. This can happen directly through positive interactions with the other members of the microbiome or indirectly by benefitting from the interactions between the other microbiome members and the host. We draw attention to the fact that the latter aspect differs from the classical Hutchinson niche concept, in that in our case the environment, i.e. the host, has the potential to change its interactions depending on the specific bacterial colonizers. Our finding also highlights the importance of the low frequency community members in shaping the overall community composition, as has recently been suggested for *Hydra* (Deines et al., 2020).

For linking the community composition in *Hydra*'s microbiome to specific characteristics, we used a trait-based approach focusing on traits potentially involved in microbiome assembly and stability (summarized in Figure 6). We draw your attention to the fact that all traits were assessed through commonly used *in vitro*

405 assays. While this excludes interference by the host, the *in vitro* assays might not
406 accurately reflect each bacterial trait in the host context as they might depend on and
407 change based on the very specific external conditions that cannot be accurately
408 mimicked with *in vitro* assays (nevertheless also note the examples given below
409 where performance of the microbiota in the *in vitro* assays was positively associated
410 with performance in the host).
411 A first step in microbiome assembly is the attachment to host surfaces, which
412 can happen in a multitude of ways. In the human intestine, for example, microbes
413 have been found to bind to mucin, a major component of the human mucosa (de Vos,
414 2015). Adhesion is thus thought to be a powerful mechanism for exerting both,
415 positive and negative selection for or against specific microbes (McLoughlin et al.,
416 2016; Schluter et al., 2015). Amongst others (van Loosdrecht et al., 1987), bacterial
417 cell surface hydrophobicity has been shown to play a crucial role in surface
418 attachment (Krasowska and Sigler, 2014). In general, hydrophobic cells adhere more
419 strongly to hydrophobic surfaces and vice versa (Giaouris et al., 2009; Kochkodan et
420 al., 2008). Nevertheless, the heterogeneity of a bacterial population needs to be taken
421 into account. For example, the presence of both, hydrophilic and hydrophobic cells,
422 have been observed in planktonic bacteria cell populations, implying that only part of
423 the population participates in an adhesion process to substrates (Krasowska and
424 Sigler, 2014). We also observe mixed cell populations for most of *Hydra*'s microbial
425 associates, except for two species, *Curvibacter* sp. and *Pelomonas* sp., which only
426 consist of hydrophilic cells. They seem to be perfectly adapted to *Hydra*'s epithelial
427 cells, which are coated with a carbohydrate-rich layer, the glycocalyx (Ouwerkerk et
428 al., 2013; Schröder and Bosch, 2016). The microbiome inhabits the outer mucus-like
429 layer of the glycocalyx (Fraune et al., 2015), which is hydrophilic. Thus, hydrophilic
430 bacterial cells should adhere more strongly to *Hydra* than hydrophobic cells. Both,
431 *Curvibacter* sp. and *Pelomonas* sp., have been shown to be of particular importance to
432 the host. *Curvibacter* sp. shows signs of coevolution with its host and contributes to
433 fungal resistance against the filamentous fungus *Fusarium* (Fraune et al., 2015).
434 *Pelomonas* sp. has been shown to be of central importance in modulating the
435 spontaneous body contractions in *Hydra* (Murillo-Rincón et al., 2017). So both
436 species contribute to host fitness, providing the opportunity for the speculation that
437 the host actively selects for specific microbes. This could happen, for example, by
438 controlling the production and release of adhesive molecules from the host epithelium
439 as suggested by McLoughlin et al. (2016).
440 After successful attachment, bacteria need to colonize the habitat. In most
441 cases, this happens through the formation of biofilms, as has been reported for the gut
442 (de Vos, 2015; Kania et al., 2007). The biofilm succeeds the planktonic phase in the
443 bacterial life cycle (McDougald et al., 2012) and represents a key ecological process
444 for the colonization of different habitats. Thus, the difference in the ability to form
445 biofilms could provide an explanation for why one species outcompetes the other
446 species or has a higher chance of persistence in the *Hydra* ecosystem. Further,
447 biofilms have been shown to protect bacterial cells from various environmental
448 stressors (Flemming and Wingender, 2010). Interestingly, from the six species tested
449 here, the one with the highest ability to form biofilms is *Pelomonas* sp., whereas the
450 two main colonizers, *Curvibacter* sp. and *Duganella* sp. show a reduced capacity to
451 form biofilms. Our finding indicates that the capability of biofilm formation is not a
452 good predictor of the bacterial performance in the *Hydra* habitat. Nevertheless, it
453 might be of importance for the establishment and persistence of some of the low
454 abundance species, such as *Pelomonas* sp. and *Acidovorax* sp..

455 Importantly, microbiomes on external surfaces of metaorganisms, such as the
456 skin, have been reported to be highly stable despite their constant exposure to
457 extrinsic factors (Oh et al., 2016). Whereas bacterial diversity is widely recognized in
458 leading to temporal stability of ecosystem processes (Bell et al., 2009; Griffin et al.,
459 2009; Prosser et al., 2007), the influence of resource niche breadth has received little
460 scientific attention (Hunting et al., 2015). Recent work studying the decomposition of
461 organic matter in experimental microcosms found that the higher the overlap in
462 resource niches, the higher the stability of the microbial community. It is reasonable
463 to assume that the same underlying principles govern stability in host-associated
464 microbial communities. We therefore measured the niche overlap and resource use of
465 the six species isolated from the *Hydra* microbiome. Interestingly, we find the niche
466 overlap between all pairwise combinations to be between 60 and 80%, with about
467 20% of the carbon sources being metabolized by all species. This suggests that
468 metabolic overlap could be involved in promoting the extreme temporal stability of
469 *Hydra*'s microbiome (Fraune and Bosch, 2007) in addition to active manipulation by
470 *Hydra* through the secretion of antimicrobial peptides and neuropeptides
471 (Franzenburg et al., 2013; Augustin et al., 2017). We also found the two main
472 colonizers, *Curvibacter* sp. and *Duganella* sp. together with *Pseudomonas* sp., to
473 possess the widest resource niche breadth of all species, and that five out of six
474 species were able to metabolize more than 50% of the 95 offered carbon substrates.
475 Overall, the relative niche breadth observed in the tested species can serve as a proxy
476 of the metabolic diversity of the *Hydra* microbiome. In the metaorganism *Hydra* it
477 seems that niche breadth of its symbionts is a fairly good indicator for relative
478 microbial performance as compared to the other members of the community, and thus
479 of the realized niche (Figure 6). This is not the case for *Pseudomonas* sp., which
480 despite its observed niche breadth, does not seem to play a major role as part of
481 *Hydra*'s microbiome. One reason for this might stem from the fact that *Pseudomonas*
482 sp. is an ubiquitous bacterium, which is generally characterized by its ability to
483 colonize all major environments and might well be the bacterial species with the
484 broadest ecological niche range (Spiers et al., 2000).
485 The metabolic overlap, i.e. redundancy, within *Hydra*'s microbial community
486 indicates that the individual species are not occupying a specific metabolic niche.
487 Nevertheless, the only one for which we observed a specific carbon usage pattern is
488 the main colonizer *Curvibacter* sp., which utilizes eight carbon sources that are not
489 metabolized by any other tested microbiome members. Whether this hints at the
490 occupation of a specific niche within *Hydra*'s microbial community and can be linked
491 to the observation that its realized is bigger than its fundamental niche is currently
492 open to speculation. An alternative option might be that *Curvibacter* sp. is
493 auxotrophic in producing certain amino acids (four of the uniquely used carbon
494 sources are the amino acids L-Leucine, L-Phenylalanine, L-Pyroglutamic Acid, and
495 D-Serine), as are 98% of all sequenced microbes (Zengler and Zaramela, 2018).
496 *Curvibacter* sp. might thus rely on the uptake of external substrates that might not be
497 secreted by the host but by its fellow community members. Analyzing the metabolic
498 interactions within this microbial network will be essential for understanding
499 community assembly, composition, and maintenance.
500 In summary we find that the here measured bacterial traits vary across
501 microbiome members. Further, the dominant species in the microbiome do not
502 necessarily perform best in all of the measured traits. We rather observe that all
503 species, independent of their density, perform well in a subset of traits, likely
504 facilitating the coexistence of several niches within the host ecosystem. Whether a

change in the realized niche of microbes can be linked to potential for dysbiosis is an interesting aspect, which warrants further investigation.

Ethics statement

Ethical restrictions do not apply to cnidarian model organisms such as *Hydra*.

Author contributions

PD and KH designed the experiments. PD performed the experiments. PD and KH analysed the data. PD, KH and TB wrote the paper.

Funding

PD received funding from the European Union's Framework Programme for Research and Innovation Horizon 2020 (2014–2020) under the Marie Skłodowska-Curie Grant Agreement No. 655914 and KH under the Marie Skłodowska-Curie Grant Agreement No. 657096. Both also received a Reintegration Grant from the Deutscher Akademischer Austausch Dienst (DAAD). This work was further supported by the Deutsche Forschungsgemeinschaft (DFG) Collaborative Research Centre (CRC) 1182 ("Origin and Function of Metaorganisms").

Acknowledgements

TB gratefully appreciates support from the Canadian Institute for Advanced Research (CIFAR) and thanks the Wissenschaftskolleg (Institute of Advanced Studies) in Berlin for a sabbatical leave.

Competing Interests

The authors declare no conflict of interest.

532 **References**

533 Augustin, R., Schröder, K., Murillo-Rincón, A. P., Fraune, S., Anton-Erxleben, F.,
534 Herbst, E.-M., et al. (2017). A secreted antibacterial neuropeptide shapes the
535 microbiome of *Hydra*. *Nat. Commun.* 8:698. doi:10.1038/s41467-017-00625-1.

536 Bell, T., Gessner, M. O., Griffiths, R. I., McLaren, J. R., Morin, P. J., and van der
537 Heijden, M. (2009). "Microbial diversity and ecosystem functioning under
538 controlled conditions and in the wild," in *Biodiversity, Ecosystem Functioning,*
539 *and Human Wellbeing*, eds. S. Naeem, D. E. Bunker, A. Hector, M. Loreau, and
540 C. P. Perring (Oxford, UK), 121–133.

541 Borecká-Melkusová, S., and Bujdáková, H. (2008). Variation of cell surface
542 hydrophobicity and biofilm formation among genotypes of *Candida albicans* and
543 *Candida dubliniensis* under antifungal treatment. *Can.J. Microbiol.* 54, 718–724.
544 doi:10.1139/w08-060.

545 Bosch, T. C. G. (2013). Cnidarian-microbe interactions and the origin of innate
546 immunity in metazoans. *Annu. Rev. Microbiol.* 67, 499–518.
547 doi:10.1146/annurev-micro-092412-155626.

548 Daou, L., Luglia, M., Périssol, C., Calvert, V., and Criquet, S. (2017). Sporulation and
549 physiological profiles of bacterial communities of three Mediterranean soils
550 affected by drying-rewetting or freezing-thawing cycles. *Soil Biol. Biochem.* 113,
551 116–121. doi:10.1016/j.soilbio.2017.06.008.

552 de Vos, W. M. (2015). Microbial biofilms and the human intestinal microbiome. *NPJ*
553 *Biofilms Microbiomes* 1, 15005. doi:10.1038/npjbiofilms.2015.5.

554 Deines, P., and Bosch, T. C. G. (2016). Transitioning from microbiome composition
555 to microbial community interactions: the potential of the metaorganism *Hydra* as
556 an experimental model. *Front. Microbiol.* 7, 1610.
557 doi:10.3389/fmicb.2016.01610.

558 Deines, P., Hammerschmidt, K., Bosch, T. C. B. (2020). Microbial species
559 coexistence depends on the host environment. *mBio* 11:e00807-20.
560 doi:10.1128/mBio.00807-20.

561 Deines, P., Lachnit, T., and Bosch, T. C. G. (2017). Competing forces maintain the
562 *Hydra* metaorganism. *Immunol. Rev.* 279, 123–136. doi:10.1111/imr.12564.

563 Falkowski, P. G., Fenchel, T., and Delong, E. F. (2008). The microbial engines that
564 drive Earth's biogeochemical cycles. *Science* 320, 1034–1039.
565 doi:10.1126/science.1153213.

566 Flemming, H. C., and Wingender, J. (2010). The biofilm matrix. *Nat. Rev. Microbiol.*
567 8, 623–633. doi:10.1038/nrmicro2415.

568 Franzenburg, S., Walter, J., Künzel, S., Wang, J., Baines, J. F., Bosch, T. C. G., et al.
569 (2013). Distinct antimicrobial peptide expression determines host species-specific
570 bacterial associations. *Proc. Natl. Acad. Sci. U.S.A.* 110, E3730–8.
571 doi:10.1073/pnas.1304960110.

572 Fraune, S., and Bosch, T. C. G. (2007). Long-term maintenance of species-specific
573 bacterial microbiota in the basal metazoan *Hydra*. *Proc. Natl. Acad. Sci. U.S.A*
574 104, 13146–13151. doi:10.1063/1.1599624.

575 Fraune, S., Anton-Erxleben, F., Augustin, R., Franzenburg, S., Knop, M., Schröder,
576 K., et al. (2015). Bacteria-bacteria interactions within the microbiota of the
577 ancestral metazoan *Hydra* contribute to fungal resistance. *ISME J.* 9, 1543–1556.
578 doi:10.1038/ismej.2014.239.

579 Giaouris, E., Chapot-Chartier, M.-P., and Briandet, R. (2009). Surface
580 physicochemical analysis of natural *Lactococcus lactis* strains reveals the
581 existence of hydrophobic and low charged strains with altered adhesive
582 properties. *Int. J. Food Microbiol.* 131, 2–9.
583 doi:10.1016/j.ijfoodmicro.2008.09.006.

584 Granato, E. T., Meiller-Legrad, T.A., and Foster, K. R. (2019). The evolution and
585 ecology of bacterial warfare. *Curr. Biol.* 29, R521–R537.
586 doi:10.1016/j.cub.2019.04.024.

587 Green, J. L., Bohannan, B. J. M., and Whitaker, R. J. (2008). Microbial biogeography:
588 from taxonomy to traits. *Science* 320, 1039–1043. doi:10.1126/science.1153475.

589 Griffin, J. N., O'Gorman, E. J., Emmerson, M. C., Jenkins, S. R., Klein, A. M., and
590 Loreau, M. (2009). "Biodiversity and the stability of ecosystem functioning," in
591 *Biodiversity, Ecosystem Functioning, and Human Wellbeing*, eds. S. Naeem, D.
592 E. Bunker, A. Hector, M. Loreau, and C. P. Perring (Oxford, UK: Oxford
593 University Press), 78–93.

594 Guittar, J., Shade, A., and Litchman, E. (2019). Trait-based community assembly and
595 succession of the infant gut microbiome. *Nat. Commun.* 10, 512.
596 doi:10.1038/s41467-019-08377-w.

597 Holt, R. D. (2009). Bringing the Hutchinsonian niche into the 21st century: ecological
598 and evolutionary perspectives. *Proc. Natl. Acad. Sci. U.S.A.* 106, 19659–19665.
599 doi:10.1073/pnas.0905137106.

600 Hunting, E. R., Vijver, M. G., van der Geest, H. G., Mulder, C., Kraak, M. H. S.,
601 Breure, A. M., et al. (2015). Resource niche overlap promotes stability of
602 bacterial community metabolism in experimental microcosms. *Front. Microbiol.*
603 6, 11512. doi:10.3389/fmicb.2015.00105.

604 Hutchinson, G. E. (1957). Concluding remarks. *Cold Spring Harb. Sym.* 22, 415–427.

605 Kania, R. E., Lamers, G. E. M., Vonk, M. J., Huy, P. T. B., Hiemstra, P. S.,
606 Bloemberg, G. V., et al. (2007). Demonstration of bacterial cells and glycocalyx
607 in biofilms on human tonsils. *Arch. Otolaryngol.* 133, 115–121.
608 doi:10.1001/archotol.133.2.115.

609 Kau, A. L., Ahern, P. P., Griffin, N. W., Goodman, A. L., and Gordon, J. I. (2011).
610 Human nutrition, the gut microbiome and the immune system. *Nature* 474, 327–
611 336. doi:10.1038/nature10213.

612 Kochkodan, V., Tsarenko, S., Potapchenko, N., Kosinova, V., and Goncharuk, V.
613 (2008). Adhesion of microorganisms to polymer membranes: a photobactericidal
614 effect of surface treatment with TiO_2. *Desalination* 220, 380–385.
615 doi:10.1016/j.desal.2007.01.042.

616 Kopac, S. M., and Klassen, J. L. (2016). Can they make it on their own? Hosts,
617 microbes, and the holobiont niche. *Front. Microbiol.* 7, 1647.
618 doi:10.3389/fmicb.2016.01647.

619 Krasowska, A., and Sigler, K. (2014). How microorganisms use hydrophobicity and
620 what does this mean for human needs? *Front. Cell. Infect. Microbiol.* 4, 653.
621 doi:10.3389/fcimb.2014.00112.

622 Krause, S., Le Roux, X., Niklaus, P. A., Van Bodegom, P. M., Lennon, J. T.,
623 Bertilsson, S., et al. (2014). Trait-based approaches for understanding microbial
624 biodiversity and ecosystem functioning. *Front. Microbiol.* 5, 2019.
625 doi:10.3389/fmicb.2014.00251.

626 Leibold, M. A. (1995). The niche concept revisited: mechanistic models and
627 community context. *Ecology* 76, 1371–1382. doi:10.2307/1938141.

628 Lenhoff, H. M., and Brown, R. D. (1970). Mass culture of *Hydra*: an improved
629 method and its application to other aquatic invertebrates. *Lab. Anim.* 4, 139–154.
630 doi:10.1258/002367770781036463.

631 Louca, S., Polz, M. F., Mazel, F., Albright, M. B. N., Huber, J. A., O'Connor, M. I.,
632 et al. (2018). Function and functional redundancy in microbial systems. *Nat. Ecol.*
633 *Evol.* 2, 936–943. doi:10.1038/s41559-018-0519-1.

634 Martiny, J. B. H., Jones, S. E., Lennon, J. T., and Martiny, A. C. (2015). Microbiomes
635 in light of traits: a phylogenetic perspective. *Science* 350, aac9323–aac9323.
636 doi:10.1126/science.aac9323.

637 Materna, A. C., Friedman, J., Bauer, C., David, C., Chen, S., Huang, I. B., et al.
638 (2012). Shape and evolution of the fundamental niche in marine *Vibrio*. *ISME J.*
639 6, 2168–2177. doi:10.1038/ismej.2012.65.

640 McDougald, D., Rice, S. A., Barraud, N., Steinberg, P. D., and Kjelleberg, S. (2012).
641 Should we stay or should we go: mechanisms and ecological consequences for
642 biofilm dispersal. *Nat. Rev. Microbiol.* 10, 39–50. doi:10.1038/nrmicro2695.

643 McFall-Ngai, M., Hadfield, M. G., Bosch, T. C. G., Carey, H. V., Domazet-Loso, T.,
644 Douglas, A. E., et al. (2013). Animals in a bacterial world, a new imperative for
645 the life sciences. *Proc. Natl. Acad. Sci. U.S.A.* 110, 3229–3236.
646 doi:10.1073/pnas.1218525110.

647 McLoughlin, K., Schluter, J., Rakoff-Nahoum, S., Smith, A. L., and Foster, K. R.
648 (2016). Host selection of microbiota via differential adhesion. *Cell Host Microbe*
649 19, 550–559. doi:10.1016/j.chom.2016.02.021.

650 Murillo-Rincón, A. P., Klimovich, A., Pemöller, E., Taubenheim, J., Mortzfeld, B.,
651 Augustin, R., et al. (2017). Spontaneous body contractions are modulated by the

652 microbiome of *Hydra*. *Sci. Rep.* 7, 15937. doi:10.1038/s41598-017-16191-x.

653 Oh, J., Byrd, A. L., Park, M., NISC Comparative Sequencing Program, Kong, H. H.,
654 and Segre, J. A. (2016). Temporal stability of the human skin microbiome. *Cell*
655 165, 854–866. doi:10.1016/j.cell.2016.04.008.

656 Ouwerkerk, J. P., de Vos, W. M., and Belzer, C. (2013). Glycobiome: bacteria and
657 mucus at the epithelial interface. *Best Pract. Res. Cl. Ga.* 27, 25–38.
658 doi:10.1016/j.bpg.2013.03.001.

659 Pearman, P. B., Guisan, A., Broennimann, O., and Randin, C. F. (2008). Niche
660 dynamics in space and time. *Trends Ecol. Evol.* 23, 149–158.
661 doi:10.1016/j.tree.2007.11.005.

662 Peeters, E., Nelis, H. J., and Coenye, T. (2008). Comparison of multiple methods for
663 quantification of microbial biofilms grown in microtiter plates. *J. Microbiol.*
664 *Meth.* 72, 157–165. doi:10.1016/j.mimet.2007.11.010.

665 Pocheville, A. (2015). "The ecological niche: history and recent controversies," in
666 *Handbook of Evolutionary Thinking in the Sciences*, eds. T. Heams, P. Huneman,
667 G. Lecointre, and M. Silberstein (Dordrecht: Springer, Dordrecht), 547–586.
668 doi:10.1007/978-94-017-9014-7_26.

669 Prosser, J. I., Bohannan, B. J. M., Curtis, T. P., Ellis, R. J., Firestone, M. K.,
670 Freckleton, R. P., et al. (2007). The role of ecological theory in microbial
671 ecology. *Nat. Rev. Microbiol.* 5, 384–392. doi:10.1038/nrmicro1643.

672 Quinn, G. P., and Keough, M. J., (2003). Experimental Design and Data Analysis for
673 Biologists. Cambridge: Cambridge University Press.
674
675 Rausch, P., Rühlemann, M., Hermes, B. M., Doms, S., Dagan, T., Dierking., K., et al.
676 (2019). Comparative analysis of amplicon and metagenomic sequencing methods
677 reveals key features in the evolution of animal metaorganisms. *Microbiome*
678 7:133. doi:10.1186/s40168-019-0743-1.

679 Ren, D., Madsen, J. S., Sørensen, S. J., and Burmølle, M. (2015). High prevalence of
680 biofilm synergy among bacterial soil isolates in cocultures indicates bacterial
681 interspecific cooperation. *ISME J.* 9, 81–89. doi:10.1038/ismej.2014.96.

682 Rosenberg, M. (1984). Bacterial adherence to hydrocarbons: a useful technique for
683 studying cell surface hydrophobicity. *FEMS Microbiol Lett* 22, 289–295.
684 doi:10.1111/j.1574-6968.1984.tb00743.

685 RStudio Team (2015). *RStudio: Integrated Development for R (RStudio, Inc., Boston,*
686 *MA)*. Available at: Available at https://www.rstudio.com.

687 Schluter, J., Nadell, C. D., Bassler, B. L., and Foster, K. R. (2015). Adhesion as a
688 weapon in microbial competition. *ISME J.* 9, 139–149.
689 doi:10.1038/ismej.2014.174.

690 Schröder, K., and Bosch, T. C. G. (2016). The origin of mucosal immunity: lessons
691 from the holobiont *Hydra*. *mBio* 7, e01184–16. doi:10.1128/mBio.01184-16.

692 Spiers, A. J., Buckling, A., and Rainey, P. B. (2000). The causes of *Pseudomonas*
693 diversity. *Microbiology* 146, 2345–2350.

694 van Loosdrecht, M. C., Lyklema, J., Norde, W., Schraa, G., and Zehnder, A. J.
695 (1987). The role of bacterial cell wall hydrophobicity in adhesion. *Appl. Environ.*
696 *Microb.* 53, 1893–1897.

697 Vaz Jauri, P., Bakker, M. G., Salomon, C. E., and Kinkel, L. L. (2013). Subinhibitory
698 antibiotic concentrations mediate nutrient use and competition among soil
699 streptomyces. *PLoS ONE* 8, e81064. doi:10.1371/journal.pone.0081064.

700 Wein, T., Dagan, T., Fraune, S., Bosch, T. C. G., Reusch, T. B. H., and Hülter, N. F.
701 (2018). Carrying capacity and colonization dynamics of *Curvibacter* in the *Hydra*
702 host habitat. *Front. Microbiol.* 9, 185. doi:10.3389/fmicb.2018.00443.

703 Wennekes, P. L., Rosindell, J., and Etienne, R. S. (2012). The neutral-niche debate: a
704 philosophical perspective. *Acta Biotheor.* 60, 257–271. doi:10.1007/s10441-012-
705 9144-6.

706 Whittaker, R. H., Levin, S. A., and Root, R. B. (1973). Niche, habitat, and ecotope.
707 *Am. Nat.* 107, 321–338. doi:10.1086/282837;subPage:string:Access.

708 Zengler, K., and Zaramela, L. S. (2018). The social network of microorganisms - how
709 auxotrophies shape complex communities. *Nat. Rev. Microbiol.* 16, 383–390.
710 doi:10.1038/s41579-018-0004-5.

711
712

713 **Figures**

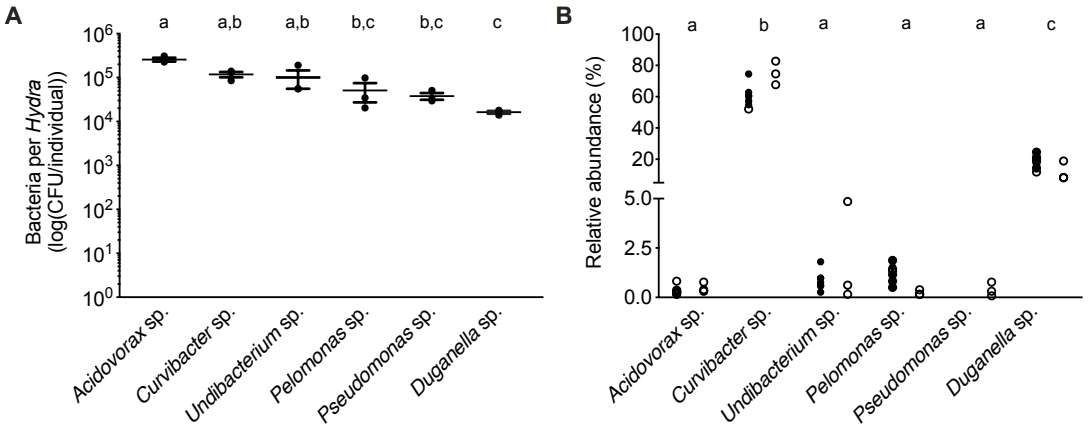

714
715 **Figure 1.** Performance of the six main bacterial colonizers isolated from the *Hydra*
716 microbiome. (**A**) Carrying capacity of the *Hydra* ecosystem during mono-associations
717 of germ-free polyps with individual bacterial species. Error bars are s.e.m., based on
718 n=3. (**B**) Relative read abundances (%) of the different bacterial colonizers in wild-
719 type (open circles) and conventionalized polyps (filled circles), compiled from
720 previously published studies (left: (Murillo-Rincón et al., 2017), right: (Franzenburg
721 et al., 2013)). Statistical differences as determined by post hoc tests ($P < 0.05$) are
722 indicated by the different letters.
723
724
725

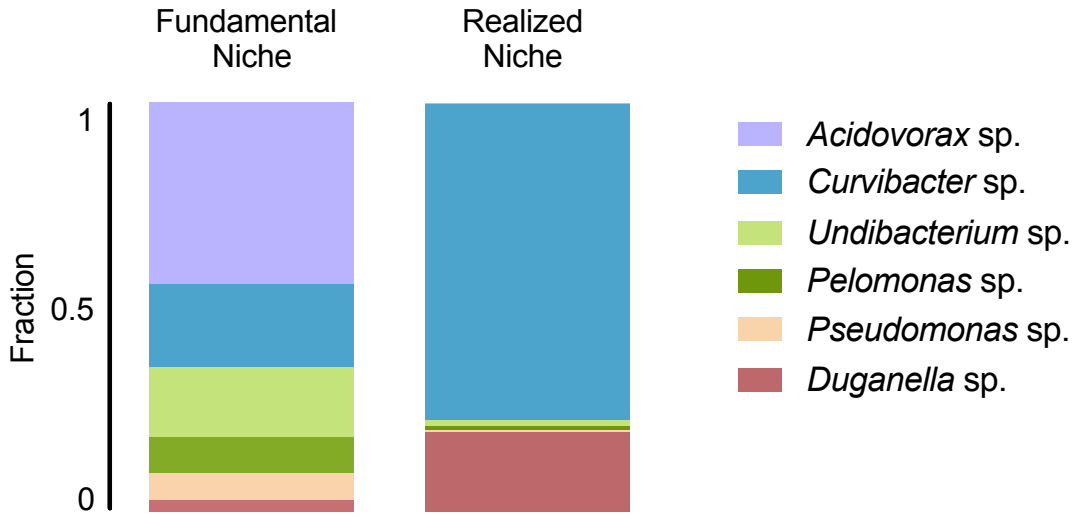

726
727 **Figure 2.** Fundamental and realized niches of six members of *Hydra*'s microbiome
728 (based on mono-colonization's and microbial community composition). The realized
729 niche includes additional constrains arising from inter-specific competition between
730 microbiome members.

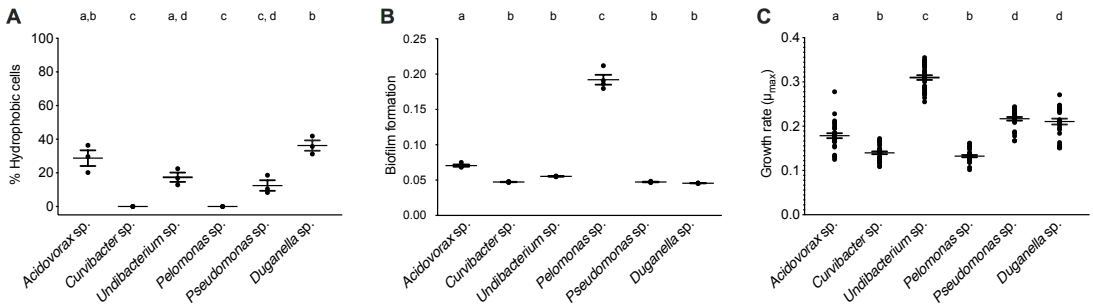

Figure 3. Trait measures of bacterial species isolated from the *Hydra* microbiome. (**A**) Cell surface hydrophobicity (Error bars are s.e.m., n=3), and (**B**) Biofilm formation capacity of six bacterial isolates. Error bars are s.e.m., n=4. (**C**) Bacterial growth rates of individual species measured *in vitro*. Error bars are s.e.m., based on n=30. Statistical differences as determined by post hoc tests ($P < 0.05$) are indicated by the different letters.

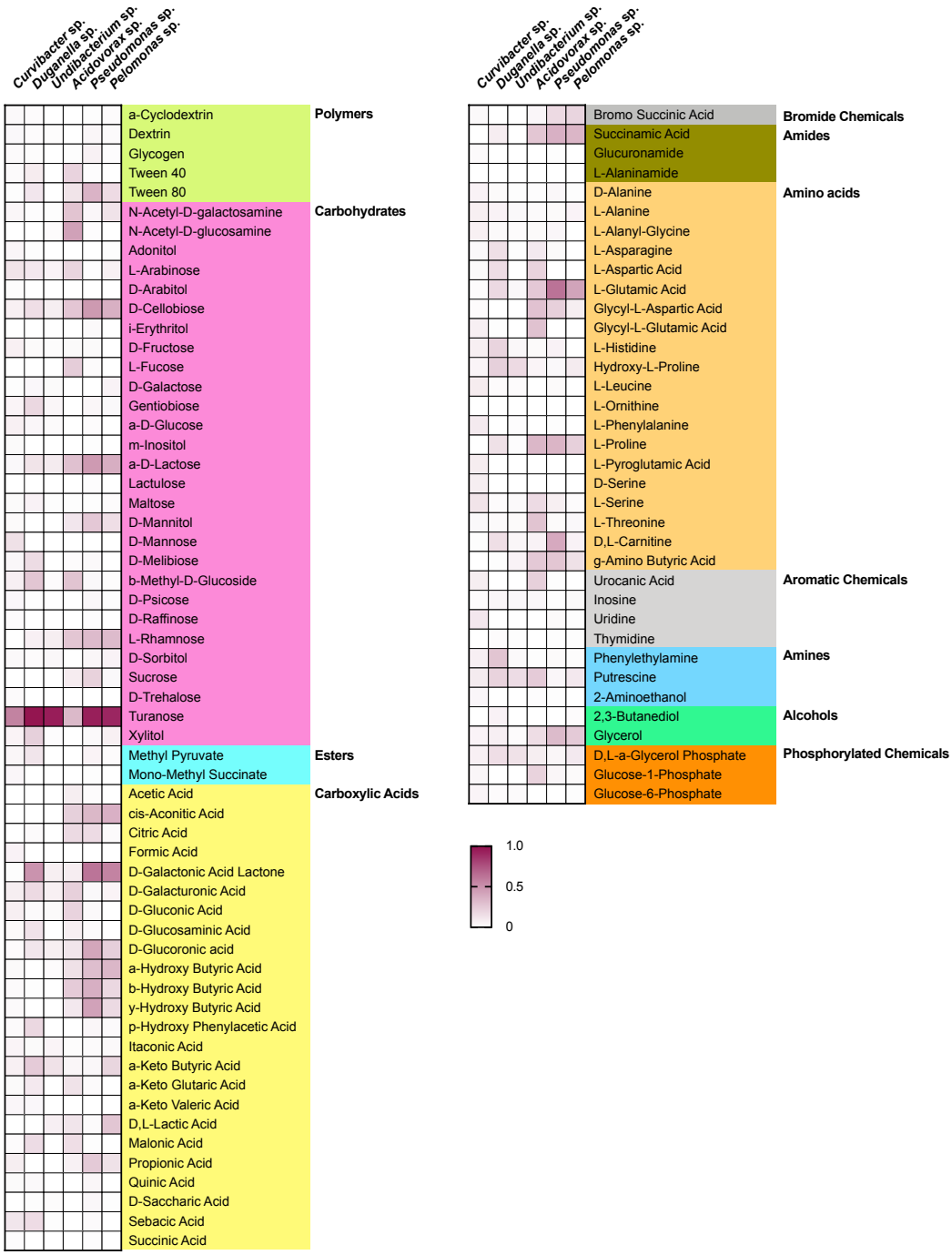

Figure 4. Substrate utilization pattern of six bacterial isolates from the *Hydra* microbiome measured with a BIOLOG assay. Colors indicate the relative magnitude of substrate utilization.

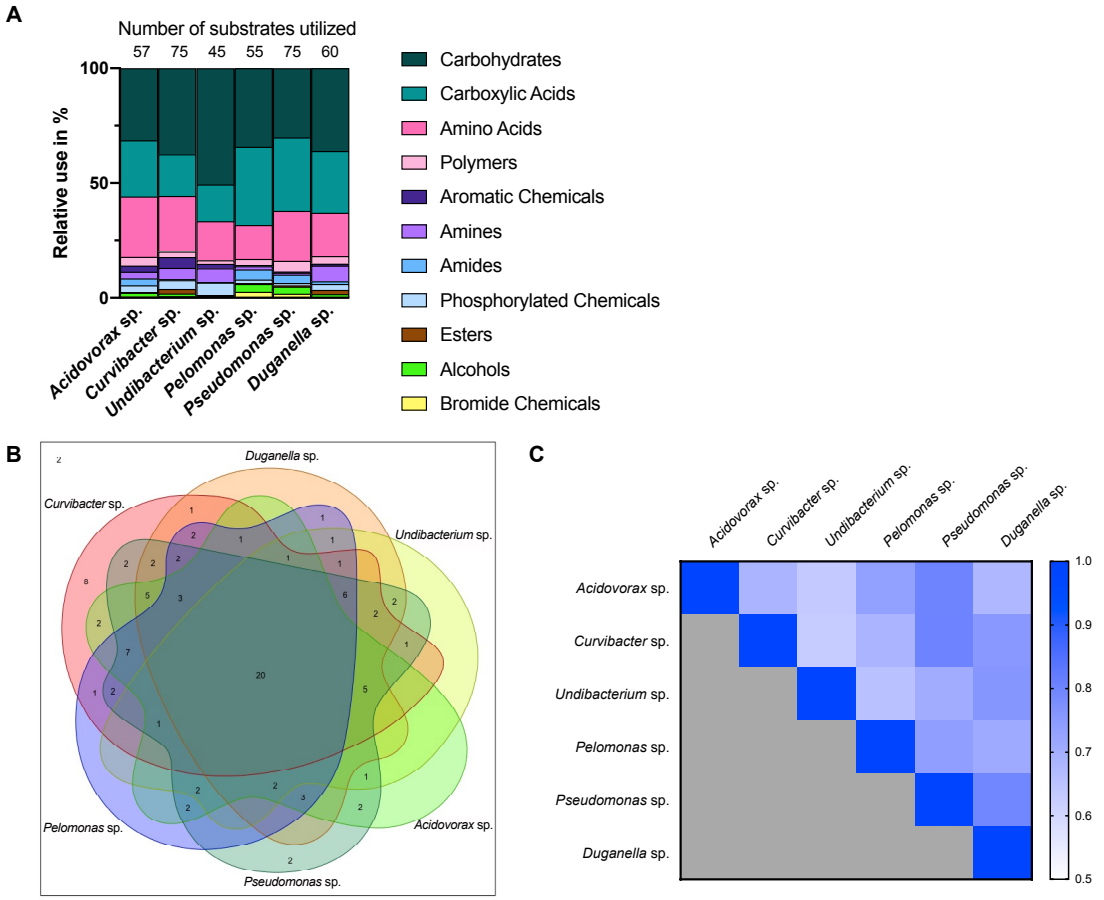

Figure 5. Metabolic phenotype diversity in *Hydra*'s microbiome. (**A**) Number of substrates utilized (out of 95) and their relative use (%). (**B**) Venn diagram showing the distribution of shared substrates among the microbiome members. (**C**) Niche overlap among all pairwise combinations of six *Hydra* microbiome members. A value of 1 indicates the use of the same nutrients (100% overlap) and 0 indicates no nutrient overlap.

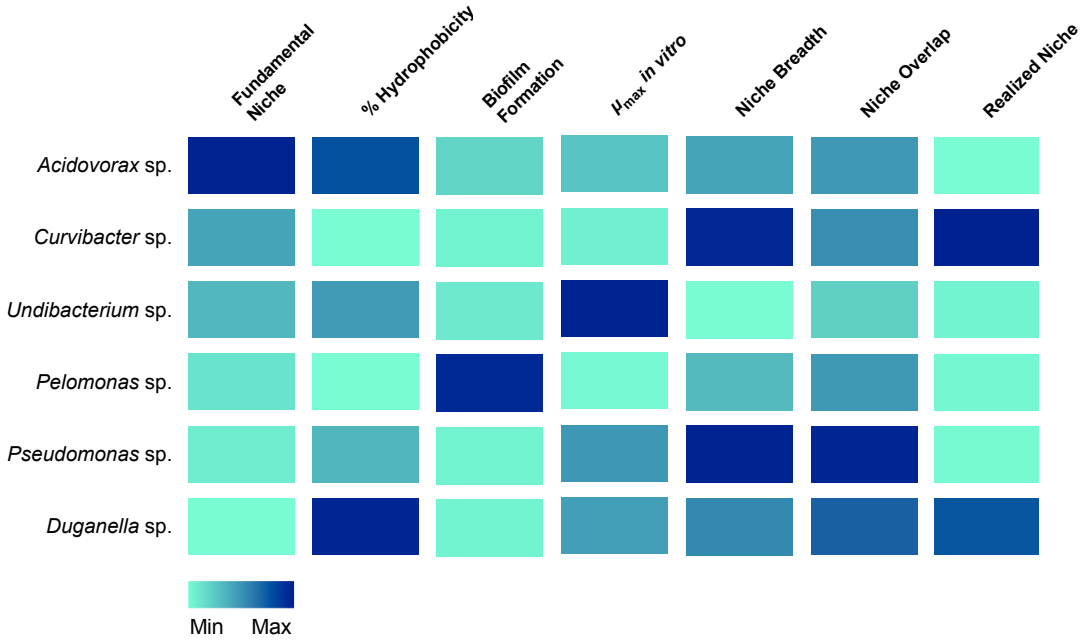

Figure 6. Association of traits with the occupation of the fundamental and realized niches in *Hydra*'s six microbiome members. Colors indicate the relative magnitude of the respective trait.